Journal of Biomolecular NMR, **12:** 373–383, 1998.
KLUWER/ESCOM

Sensitivity optimized HCN and HCNCH experiments for $^{13}C/^{15}N$ labeled oligonucleotides

Radovan Fiala[a], Feng Jiang[b] and Vladimír Sklenář[a]
[a]*Laboratory of Biomolecular Structure & Dynamics, Masaryk University, Kotlářská 2, CZ-611 37 Brno, Czech Republic;* [b]*Cellular Biochemistry and Biophysics Program, Memorial Sloan-Kettering Cancer Center, 1275 York Avenue, New York, NY 10021, U.S.A.*

Received 19 January 1998; Accepted 18 May 1998

Key words: assignment, labeled RNA, oligonucleotide, triple resonance

Abstract

Triple resonance HCN and HCNCH experiments used in studies of $^{13}C/^{15}N$ labeled oligonucleotides include extended evolution periods (typically up to 100 ms) to allow coherence transfer through a complex heteronuclear spin network. Unfortunately, most of the magnetization is lost during the evolution due to fast spin–spin relaxation dominated by one-bond $^{1}H–^{13}C$ dipolar interaction. As demonstrated recently, the sensitivity of the experiments can be dramatically improved by keeping the spin system in a state of proton–carbon multiple-quantum coherence, which is not affected by the strong dipolar coupling. However, the multiple-quantum coherence is very sensitive to homonuclear as well as long-range heteronuclear interactions. Unwanted magnetization transfer due to these interactions can reduce the sensitivity back to the level of a single-quantum experiment and, for some spin moieties, even eliminate the signal completely. In the present paper we show that a modified HCN scheme that refocuses the interfering coherences improves sensitivity routinely by a factor of 1.5 to 4 over a nonselective experiment. In addition, novel multiple-quantum 2D and 3D HCNCH experiments with substantially enhanced sensitivity are presented.

Introduction

Traditionally, the assignment of proton resonances in oligonucleotides has relied mainly on through-space interactions due to the nuclear Overhauser effect (NOE) (Wüthrich, 1986). As the through-space interactions necessarily depend on conformation, the results have often been ambiguous and an independent confirmation was highly desirable. The advent of techniques for the preparation of ^{13}C- and ^{15}N-labeled RNA (Nikonowicz et al., 1992; Batey et al., 1992; Michnicka et al., 1993) has allowed the use of heteronuclear through-bond correlation techniques for this purpose. Triple resonance experiments have been proposed for sugar-base correlations (Farmer et al., 1993; Sklenář et al., 1993: Sklenář et al., 1993a; Farmer et al., 1994; Tate et al. 1994), for sequential backbone assignments (Heus et al., 1994; Marino et al., 1994; Wijmenga et al., 1995; Marino et al., 1995; Tate et al., 1995; Varani et al., 1995; Ramachandran et al., 1996), and for correlating exchangeable and non-exchangeable protons in pyrimidine (Simorre et al., 1995) and purine bases (Fiala et al., 1996; Sklenář et al., 1996; Simorre et al., 1996, Simorre et al., 1996a). For optimum polarization transfer between nuclei X and Y with a coupling constant J_{XY}, an evolution delay of length $1/(2J_{XY})$ is needed. Since the heteronuclear $^{13}C–^{15}N$ coupling constants in RNA are 12 Hz or less, evolution periods of up to 100 ms are required. As a consequence, most of the signal is lost during the pulse sequence due to spin–spin relaxation. Applications of the experiments mentioned above to larger RNA oligonucleotides (more than 30 nucleotides) therefore often produced disappointing results. The dominant relaxation mechanism for ^{13}C magnetization is a large one-bond $^{1}H–^{13}C$ dipolar interaction. In the slow tumbling limit this relaxation mechanism is effectively switched off for $^{1}H–^{13}C$

zero- and double-quantum coherences (Griffey and Redfield, 1987; Grzesiek and Bax, 1995). Consequently, the signal loss due to fast relaxation can be significantly reduced in pulse schemes that produce the ^{1}H–^{13}C multiple-quantum instead of ^{13}C single-quantum coherences during prolonged evolution delays. Recent papers indeed show significant sensitivity enhancement in HCN experiments correlating H1′ hydrogen with N1/9 nitrogen for RNA oligonucleotides with more than 30 residues (Marino et al., 1997; Sklenář et al., 1998). However, the proton magnetization in the transverse plane is very sensitive to both homonuclear and long-range heteronuclear interactions. Unwanted magnetization transfer due to these interactions can reduce the benefit of slower spin-spin relaxation rates and, for some spin moieties, even eliminate the signal completely. Here we show that the sensitivity of triple-resonance **Hs**/**Hb**C**Nb** experiment which refocuses the interfering coherences is improved routinely by a factor of 1.5 to 4 over a nonselective multiple-quantum version (Marino et al. 1997).[1] A similar approach can also be used to improve the sensitivity of the **Hs**CNC**Hb** experiment (Sklenář et al., 1993) which correlates sugar H1′ and base H6/8 protons directly via H1 → C1′ → N9/1 → C8/6 → H8/6 coherence transfer. The improved sensitivity of the novel multiple-quantum **Hs**C**Nb**C**Hb** scheme enables one to run the experiment in a 3D mode with additional N1/9 chemical shift labeling to remove overlap from the 2D Hs–Hb correlation spectrum. Performance of previously published and newly developed experiments is carefully compared and demonstrated on an ATP-binding RNA aptamer complex containing 40 nucleotides.

Materials and methods

Sample preparation

The uniformly labeled RNA aptamer (Scheme 1) was enzymatically synthesized from labeled NTPs by *in vitro* transcription from a DNA template with (^{13}C,^{15}N)-labeled nucleoside triphosphates using T7 RNA polymerase and purified by gel electrophoresis (Nikonowicz et al., 1992; Batey et al., 1992). One and a half equivalents of unlabeled AMP were added to form the complex. The final sample concentration was 3.5 mM in 99.95% D2O with 10 mM sodium phosphate and 0.2 mM EDTA at pH 6.7. The sample was placed in a Shigemi sample tube and had a total volume of 270 μl. The details of the sample preparation have been published elsewhere (Jiang et al., 1996).

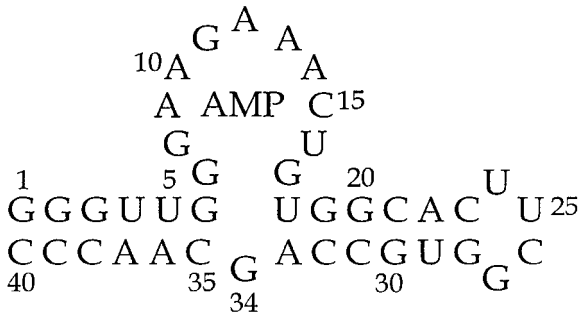

Scheme 1. The ATP-binding RNA aptamer.

NMR spectroscopy

The NMR experiments were recorded on a Bruker DRX 500 spectrometer using a triple resonance $^{1}H/^{13}C$/BB probehead equipped with a *z*-gradient coil. **Hs**/**Hb**C**Nb** experiments were recorded at 298 K and **Hs**C**Nb**C**Hb** experiments at 303 K. The schematics of the new pulse sequences are shown in Figures 1 and 2. Four pulse sequences were used to evaluate the sensitivity of various approaches to the *out-and-back* **Hs**/**Hb**C**Nb** experiments for H1′–N1/9 and H6/8–N1/9 correlations. In the original SQ experiment (single quantum, Sklenář et al., 1993a) the polarization transfer to ^{13}C leads to a single quantum coherence during the evolution interval. In the MQ_ns (multiple-quantum non-selective, Marino et al., 1997), MQ_SL (Multiple-Quantum Spin-Lock, Sklenář et al., 1998), and MQ_sel (Multiple-Quantum selective, Figure 1) experiments the absence of a proton 90 °C pulse creates zero- and double-quantum ^{1}H–^{13}C coherences. In the MQ_ns and MQ_sel pulse sequences the ^{1}H chemical shift evolution is refocused by 180° pulses, while in the MQ_SL experiment the evolution is eliminated by a spin-lock. The evolution interval Δ was set to 15 ms, except in the MQ_ns experiment where 12.5 ms is required because of the value of the $J_{C1'C2'}$ coupling constant. The parameters of shaped pulses given in the figure captions were chosen to selectively affect the nuclei indicated in the pulse schemes. For the SQ and MQ_SL experiments we used ^{13}C 2.862 ms REBURP pulse with addi-

[1] Nuclei in bold with suffix s or b denote spins on the ribose or base used for chemical shift labeling in 2D and 3D experiments, **Hs/Hb** indicates that correlation of both Hs and Hb is obtained at the same time.

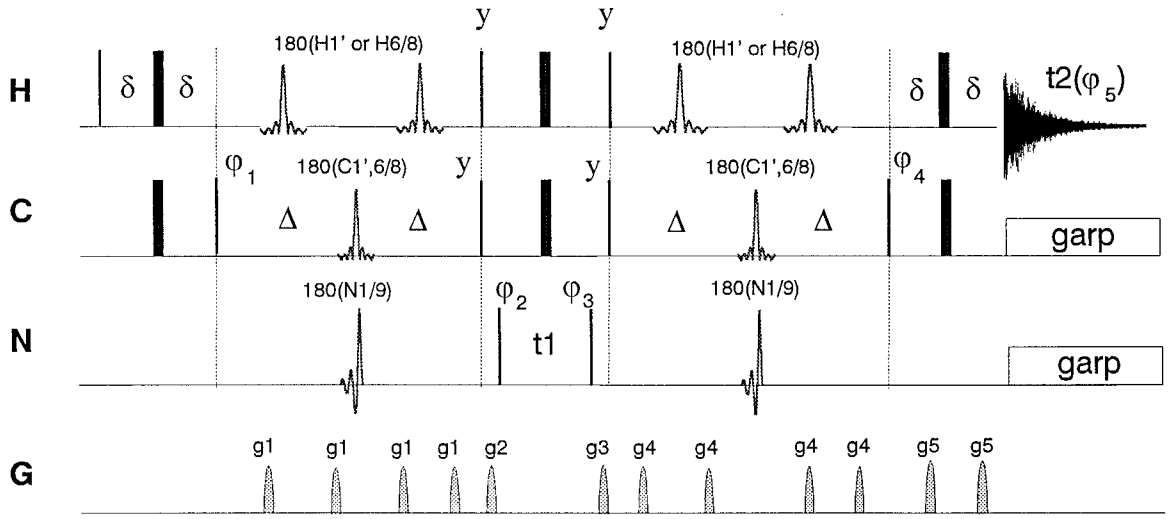

Figure 1. Pulse scheme for MQ_sel (optimized multiple-quantum selective experiment) **Hs**/**Hb**C**Nb** experiment. The thin and thick bars represent nonselective 90° and 180° pulses, respectively. The evolution delays: $\delta = 1.40$ ms as a compromised value for $J_{C1'H1'}$ and $J_{C6/8H6/8}$, $\Delta = 15$ ms. At 500 MHz the band-selective pulses were set as follows: proton 4-ms band-selective 180° REBURP pulses (Geen and Freeman, 1991) were centered at 5.7 ppm and 7.8 ppm for H1′ and H6/8 correlations, respectively; 3.0 ms REBURP centered at 90 ppm for **Hs**C**Nb** or 2.5 ms REBURP centered at 140 ppm for **Hb**C**Nb** corelations; 2.0 ms IBURP-2 on ^{15}N positioned at 158 ppm. GARP decoupling (Shaka et al., 1985) of ^{13}C and ^{15}N was used during detection. The pulses were applied along the x-axis unless otherwise specified. Phase cycling: $\varphi_1 = x, -x$; $\varphi_2 = 2(x), 2(-x)$; $\varphi_3 = 8(x), 8(-x)$; $\varphi_4 = 4(x), 4(-x)$; $\varphi_5 = abba$ where $a = x, -x, -x, x$, and $b = -x, x, x, -x$. In addition, φ_3 is incremented in States-TPPI manner to achieve quadrature detection in the F_1 dimension. Sine-bell modulated gradient pulses of 800 μs duration were applied with the strengths $g1 = 4.2$, $g2 = 2.5$, $g3 = 4.8$, $g4 = 7.2$, $g5 = 9.0$, $g6 = 8.4$ G/cm followed by 100 μs recovery delays.

tional cosine modulation ($f_m = 3144$ Hz) to provide simultaneous refocusing at 90±5.5 and 140±5.5 ppm.

In the original 2D **Hs**CNC**Hb** experiment (Sklenář et al., 1993) the single-quantum ^{13}C magnetization is generated immediately after the H1′–C1′ refocused INEPT transfer. In the multiple-quantum version (Figure 2) the double- and zero-quantum ^{1}H–^{13}C coherence is kept for a maximum allowable time during both the C1′ → N1/9 and N1/9 → C8/6 evolution. In the molecule used for this study, one of the H1′ protons (G_{28}) is shifted to 4.4 ppm, well within the H2′ region. If the proton selective pulse covers the typical range of H1′ chemical shifts the H1′ of G_{28} is not excited. Therefore, we collected two sets of data with the **Hs**CNC**Hb** pulse sequence. The proton selective refocusing pulses 180(H1) covered the range of 4.4 to 6.4 ppm in the first one and 4.7 to 6.7 ppm in the other. The corresponding results are referred to as MQ1 and MQ2 in Table 2. In the 3D **Hs**C**Nb**C**Hb** experiment (Figure 2), the second indirect ^{15}N dimension was produced by stepping the 180° nitrogen and carbon pulses in a constant time manner. The data were processed, evaluated and plotted using the XWINNMR program (Bruker). Other details important for experimental setup are either given in figure captions or specified in the Discussion section.

Results

A comparison of performance of the four pulse sequences in the sugar and base regions is shown in Figure 3. To evaluate the different modes of the **Hs**/**Hb**C**Nb** experiment quantitatively, the H1′–N1/9 and H6/8–N1/9 crosspeak intensities for two of each A, C, G, and U nucleosides were measured. Well resolved peaks were chosen for the evaluation to avoid errors resulting from peak overlap. The relative intensities of crosspeaks are given in Table 1. The sensitivity given in the table for the selective multiple-quantum experiment (MQ_sel) refers to the case when the selective pulse does not affect the H1′ proton of G_{28}. In the sugar H1′–N1/9 region, the multiple-quantum methods MQ_ns, MQ_SL and MQ_sel show sensitivity increases across the board, with the exceptions of G_{11} and G_{34}, where the sensitivity of the MQ_ns experiment is not greater than that of the SQ experiment. The MQ_sel experiment proves to be the most sensitive one. When the rela-

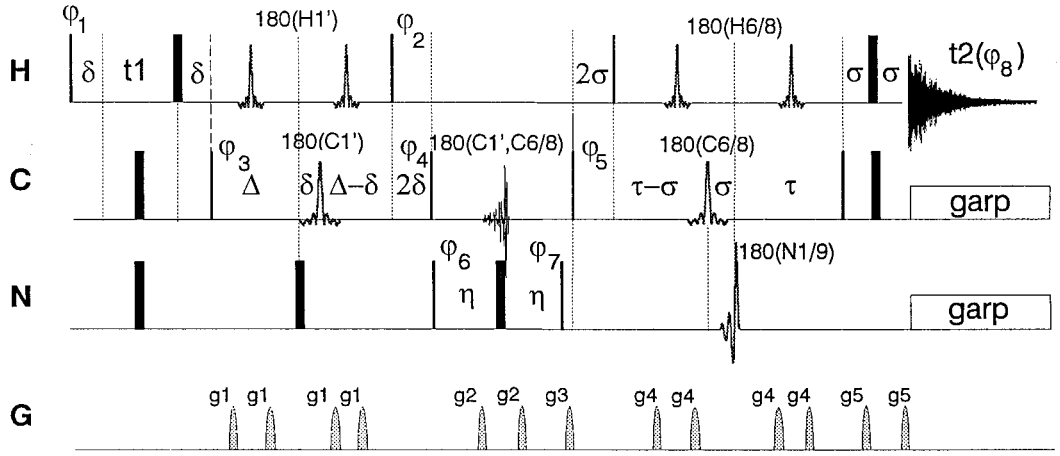

Figure 2. Pulse scheme for MQ (optimized multiple-quantum) **Hs**CNC**Hb** experiment. The evolution delays: $\delta = 1.6$ ms, $\Delta = 18.0$ ms, $\eta = 18.0$ ms, $\tau = 18.0$ ms, $\sigma = 1.25$ ms. At 500 MHz the band-selective pulse were set as follows: 180(C1′): 2.862 ms REBURP centered at 90 ppm, 180(C1′,C6/8): 3.0 ms IBURP2 pulse with additional cosine modulation ($f_m = 3144$ Hz) to provide inversion at 90±4.3 and 140±4.3 ppm, 180(C6/8): 2.862 ms REBURP centered at 140 ppm, 180(N1/9): 2.0 ms IBURP-2 pulse centered at 158 ppm, 180(H1′): 4.0 ms REBURP centered at 5.7 ppm (5.4 ppm to include G_{28}, see text for details), 180(H6/8): 4.0 ms REBURP centered at 7.8 ppm. ^{13}C and ^{15}N GARP decoupling was used during detection. The pulses were applied along the x-axis unless otherwise specified. Phase cycling: $\varphi_1 = x+$ States-TPPI; $\varphi_2 = 4(y), 4(-y)$; $\varphi_3 = 2(x), 2(-x)$; $\varphi_4 = 16(x), 16(-x)$; $\varphi_5 = x, -x$; $\varphi_6 = 32(x), 32(-x)$; $\varphi_7 = 8(x), 8(-x)$; $\varphi_8 = abba$, 2(*baab*), *abba* where $a = x, -x, -x, x$, and $b = -x, x, x, -x$. The same gradient pulses were used as in Figure 1. In a 3D version, the phase φ_6 is incremented for a States-TPPI quadrature detection in ^{15}N dimension and the delay η varied in a constant time manner.

tive sensitivity of the MQ_sel experiment is defined as 1.00 the average sugar peak intensities measured in the MQ_ns, MQ_SL and SQ experiments represent only 0.66, 0.49 and 0.18, respectively. The results in the base region differ sharply for purine and pyrimidine nucleotides. With purines, all the multiple-quantum experiments show significantly better sensitivity than the single-quantum ones. Relative to the most sensitive MQ_sel, the average peak intensities in the MQ_ns and MQ_SL experiments are 0.57 and 0.37, respectively. The lower sensitivity of MQ_SL experiment with respect to MQ_ns for purine bases is probably caused by offset effects of the proton spin-lock and by lower efficiency of the phase modulated ^{13}C REBURP pulses. With pyrimidines, the MQ_ns experiment fails to achieve even the sensitivity of the SQ experiment, with most of the peaks completely absent (Figure 3b). The MQ_SL experiment (average intensity 0.33) produces a spectrum slightly better than the SQ experiment (average intensity 0.28). Under the given acquisition parameters (total acquisition time 9 h for high S/N ratio) only the MQ_sel experiment shows all the peaks expected in this region.

A comparison of the SQ and MQ 2D **Hs**CNC**Hb** spectra (total acquisition time 12 h) is shown in Figure 4. The crosspeak intensities for well resolved crosspeaks of particular purine and pyrimidine nucleotides are summarized in Table 2. The sensitivity gain of the multiple-quantum experiment over the single-quantum one was about 27% when H1′ of G_{28} was included, and about 42% when the selective pulse did not affect the H1′ proton of G_{28}. The higher sensitivity of the MQ version allows one to detect several peaks that are very weak or absent from the SQ spectrum. As an example, the correlation peaks of A_9, A_{12}, G_7 and C_{15} are marked in Figure 4a.

Discussion

The **Hs**/**Hb**C**Nb** schemes are *out-and-back* experiments in which the magnetization is transferred from H1′ (H6/8) via C1′(C6/8) to N1/9 for chemical shift labeling. The success of the experiment is heavily dependent on the efficiency of coherence transfer through the complex spin-spin network in the ribose sugar and in the pyrimidine and purine bases. The desired coherence transfer pathways for ^{15}N chemical shift labeling can be described in terms of the product operator formalism (Sörensen et al., 1983) as

$$\begin{aligned} H1'_z \;&\rightarrow\; H1'_y \rightarrow 2H1'_xC1'_z \rightarrow 2H1'_zC1'_y \\ &\rightarrow\; 4H1'_zC1'_xN1/9_z \rightarrow 4H1'_zC1'_zN1/9_y \end{aligned}$$

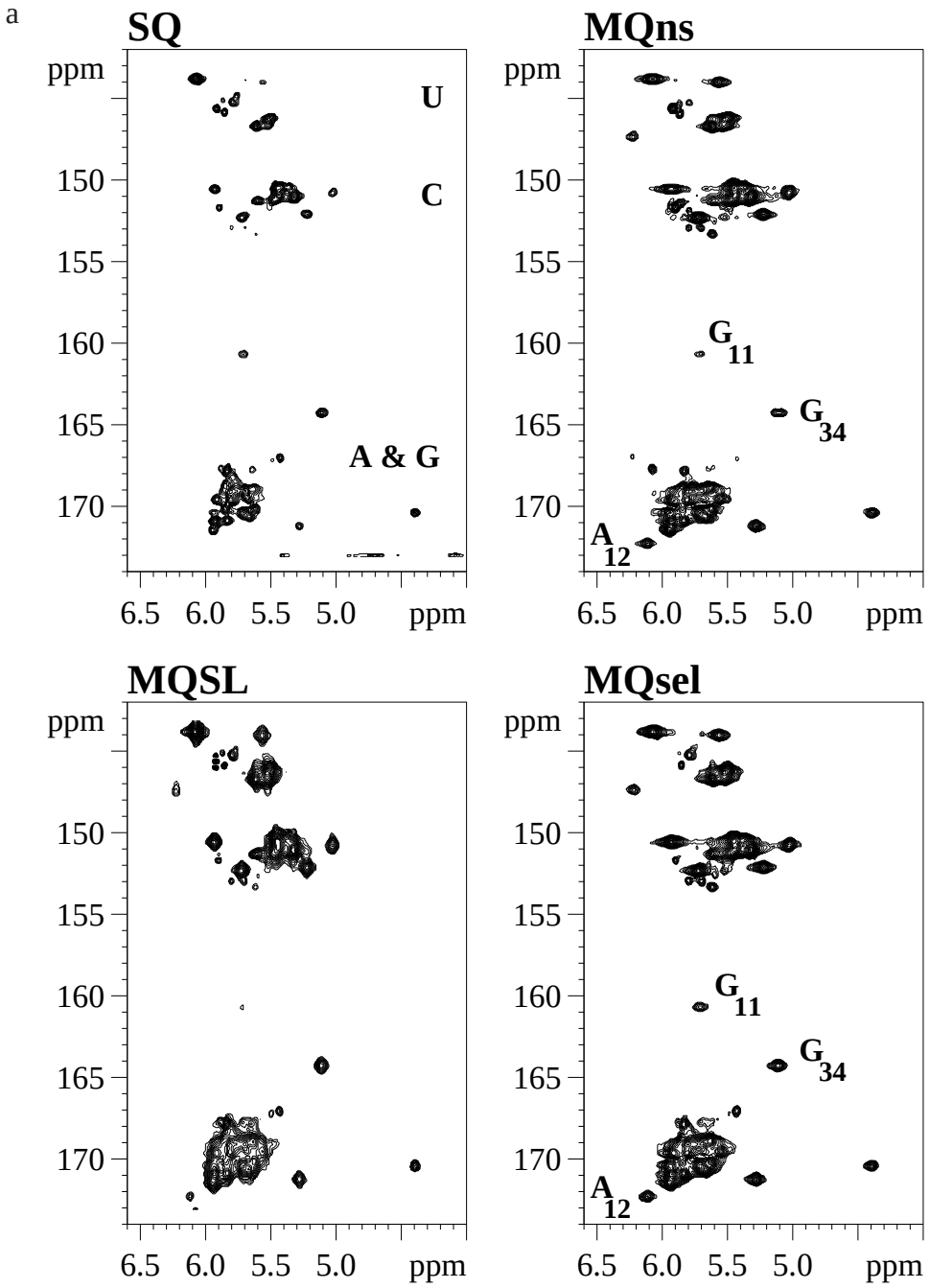

Figure 3. 500 MHz 2D ^{1}H–^{15}N correlation **Hs**/**Hb**C**Nb** spectra of ATP binding aptamer complex (Sassanfar and Shostak, 1993; Jiang et al., 1996) (Scheme 1) at 298 K, (a) H1′–N1/9 and (b) H6/8–N1/9 regions measured using SQ, MQ–ns, MQ–SL and MQ–sel experiments. The spectra were acquired with spectral widths of 5 ppm in ^{1}H and 30 ppm in ^{15}N dimensions, 96 scans per t_1 increment, 96 and 256 complex points in t_1 and t_2, respectively. The spin-lock in the MQ–SL experiment was applied with 6.45 kHz rf field and carrier frequency positioned at 6.4 ppm. The sample was 3.5 mM in 20 mM NaCl, pH 6.8. Note weak G_{11}, A_{12} and G_{34} crosspeaks in MQ–ns experiment (a) and greatly reduced or completely missing pyrimidine peaks in MQ–ns and MQ–SL experiments (b).

b

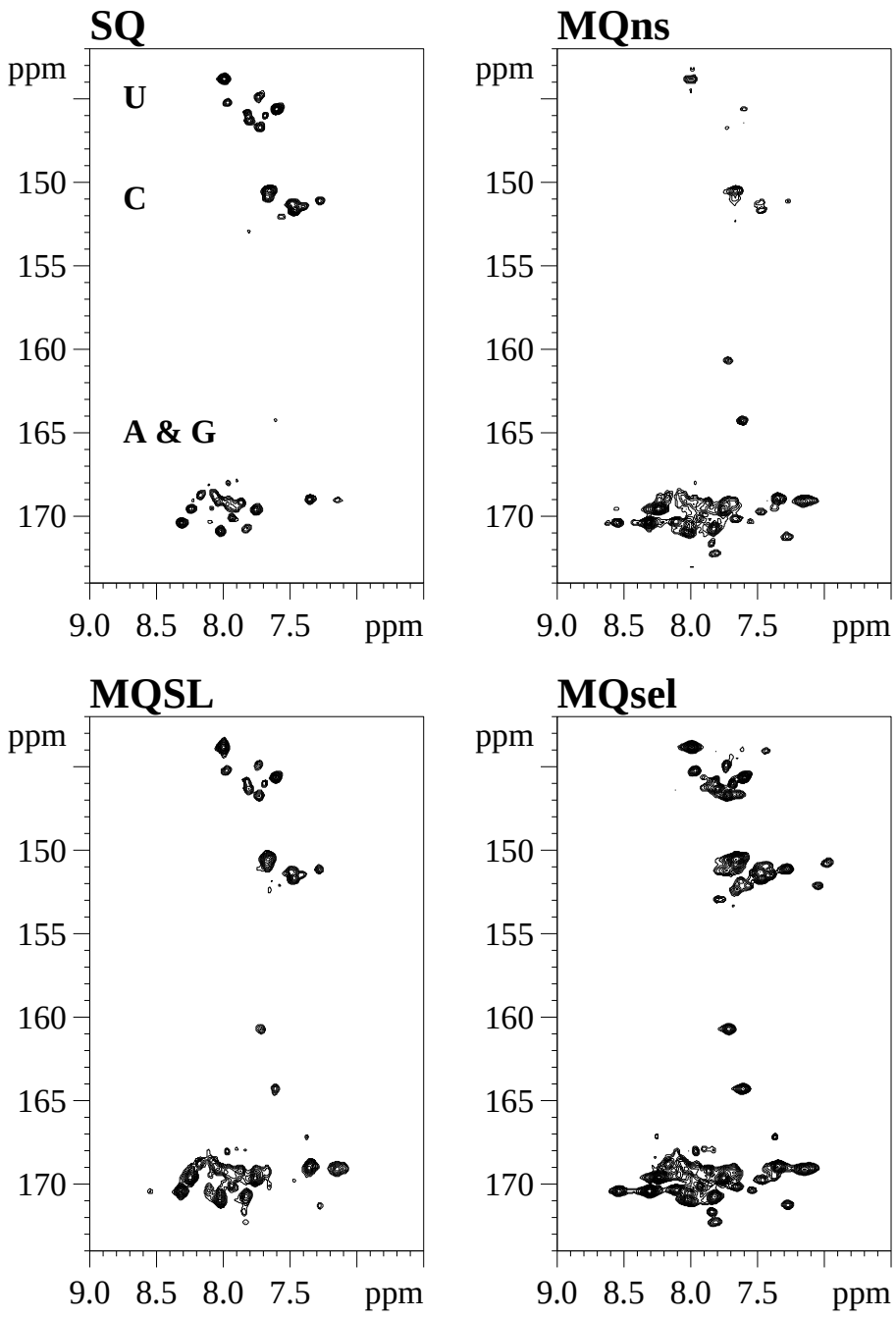

Figure 3 (continued).

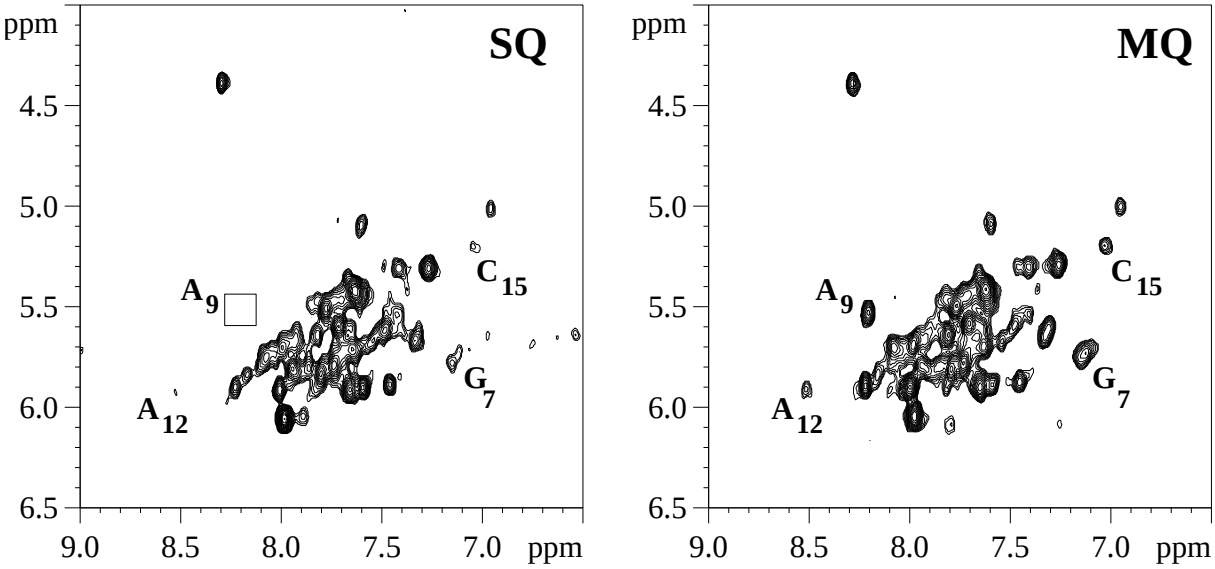

Figure 4. 500 MHz 2D ^{1}H–^{1}H **Hs**CNC**Hb** spectra correlating H1′ protons with base H6/8 protons in ATP binding aptamer complex. SQ – single-quantum experiment and MQ – multiple-quantum experiment. Spectral widths of 5 ppm in both dimension was used and 67 and 256 complex points acquired in in t_1 and t_2, respectively with 128 scans per increment. Note that the crosspeaks corresponding to the residues A_9, A_{12}, C_{15}, and G_7 are weak or missing in the SQ spectrum. Total acquisition time was 12 h.

for the sugar and

$$\begin{aligned} \mathrm{H6/8}_z \;&\rightarrow\; \mathrm{H6/8}_y \rightarrow 2\mathrm{H6/8}_x\mathrm{C6/8}_z \\ &\rightarrow\; 2\mathrm{H6/8}_z\mathrm{C6/8}_y \\ &\rightarrow\; 4\mathrm{H6/8}_z\mathrm{C6/8}_x\mathrm{N1/9}_z \\ &\rightarrow\; 4\mathrm{H6/8}_z\mathrm{C6/8}_z\mathrm{N1/9}_y \end{aligned}$$

for the bases. After t_1 encoding in the ^{15}N dimension the magnetization is transferred back by two consecutive reverse INEPT steps. The main causes of signal loss during prolonged C–N INEPT evolution delays are spin–spin relaxation and a transfer of coherence to unwanted sites. The principal competing scalar interactions are C1′–C2′ ($J_{C1'C2'} \sim 40$ Hz) in the sugar, C6–C5 ($J_{C5C6} \sim 67$ Hz) in pyrimidines and C8–C6, C8–C4 ($J_{C8C6/4} \sim 8$ Hz) and C8–N7 ($J_{C8N7} \sim 3$ Hz) in purines (Ippel et al., 1996). While the C1′–C2′ interaction can be suppressed by setting the interval 2Δ to $1/J_{C1'C2'}$ at a cost of the ability to optimize the length of 2Δ for C1′ → N1/9 transfer, the coupling network in bases is far more complex. Successful decoupling of unwanted interactions is effectively achieved by using band-selective pulses. The details for application of selective pulses in two separate single-quantum **Hs**C**Nb** and **Hb**C**Nb** experiments as well as in a **Hs/Hb**C**Nb** version have been published before (Sklenář et al., 1993a; Sklenář et al., 1998) and will not be repeated here.

In terms of relaxation, the lengths of individual sections of the pulse sequence and the state of the spin system are crucial. The longest step in the **Hs/Hb**C**Nb** pulse sequence is the coherence transfer to N1/9. Relatively small carbon-nitrogen coupling constants ($J_{C1',N1/9} \sim 11$–12 Hz, $J_{C8,N9} \sim 11$ Hz, and $J_{C6,N1} \sim 12$–13 Hz) result in theoretically optimum evolution delays for C1′–N1/9, C8–N9 and C6–N1 transfers of 42–45 ms, 45 ms, and 38–42 ms, respectively (Ippel et al., 1996). In practice, an evolution time of 25–36 ms is used to avoid excessive signal loss due to spin-spin relaxation. It is known that the principal relaxation mechanism in this step is a large one-bond ^{1}H–^{13}C dipolar interaction affecting $2\mathrm{H1'}_z\mathrm{C1'}_y$ and $2\mathrm{H6/8}_z\mathrm{C6/8}_y$ antiphase magnetizations. As described previously (Griffey and Redfield, 1987; Grzesiek and Bax, 1995), the dipolar relaxation can be effectively suppressed by creating multiple-quantum coherences involving the dipolar-coupled nuclei, namely $2\mathrm{H1'}_x\mathrm{C1'}_y$ and $2\mathrm{H6/8}_x\mathrm{C6/8}_y$ in oligonucleotides. This is easily done by moving the 90° proton pulse from the onset of the evolution period 2Δ to its end. At this point, the antiphase magnetizations $4\mathrm{H1'}_z\mathrm{C1'}_z\mathrm{N1/9}_y$, $4\mathrm{H8}_z\mathrm{C8}_z\mathrm{N1/9}_y$ and $4\mathrm{H6}_z\mathrm{C6}_z\mathrm{N1/9}_y$ are produced to allow ^{15}N chemical shift labeling. Unlike the $2\mathrm{H}_z\mathrm{C}_y$ magnetizations in the SQ pulse sequence the multi-

Table 1 Relative sensitivity of **Hs**/**HbCNb** experiments

Sugars	**SQ**	**MQ_ns**	**MQ_SL**	**MQ_sel**
U25s	0.35	0.37	0.78	1.00
U16s	0.12	0.88	0.50	1.00
C26s	0.13	0.43	0.32	1.00
C15s	0.18	0.87	0.48	1.00
G34s	0.28	0.28	0.48	1.00
G8s	0.19	0.78	0.47	1.00
A10s	0.00	0.97	0.34	1.00
A33s	0.18	0.67	0.56	1.00
Average				
Rel. to MQ_sel	**0.18**	**0.66**	**0.49**	**1.00**
Rel. to SQ	1.00	3.65	2.72	5.55
Rel. to MQ_ns	0.27	1.00	0.74	1.52
Pyrimidines	**SQ**	**MQ_ns**	**MQ_SL**	**MQ_sel**
U25b	0.48	0.11	0.44	1.00
U16b	0.00	0.41	0.23	1.00
C26b	0.36	0.19	0.36	1.00
C15b	0.28	0.25	0.33	1.00
Average				
Rel. to MQ_sel	**0.28**	**0.24**	**0.34**	**1.00**
Rel. to SQ	1.00	0.86	1.21	3.57
Rel. to MQ_ns	1.17	1.00	1.42	4.17
Purines	**SQ**	**MQ_ns**	**MQ_SL**	**MQ_sel**
G34b	0.15	0.42	0.30	1.00
G8b	0.14	0.62	0.41	1.00
A10b	0.18	0.69	0.44	1.00
A33b	0.16	0.57	0.37	1.00
Average				
Rel. to MQ_sel	**0.16**	**0.58**	**0.38**	**1.00**
Rel. to SQ	1.00	3.65	2.41	6.35
Rel. to MQ_ns	0.27	1.00	0.66	1.74
Average total				
Rel. to MQ_sel	***0.20***	***0.53***	***0.42***	***1.00***
Rel. to SQ	***1.00***	***2.67***	***2.13***	***5.01***
Rel. to MQ_ns	***0.37***	***1.00***	***0.80***	***1.88***

s – H1′N1/9 crosspeak.
b – H6N1 or H8N9 crosspeak.

Table 2. Relative sensitivity of **Hs**CNC**Hb** experiments

Adenine	**SQ**	**MQ1**	**MQ2**
A12	0.44	0.79	1.00
A13	0.49	1.01	1.00
A33	0.70	0.86	1.00
A36	0.72	0.98	1.00
Average	**0.59**	**0.91**	**1.00**
Relative to SQ	**1.00**	**1.61**	**1.78**
Guanine	**SQ**	**MQ1**	**MQ2**
G2	0.99	0.85	1.00
G34	0.77	0.71	1.00
G20	0.73	0.87	1.00
G29	0.72	0.91	1.00
Average	**0.80**	**0.83**	**1.00**
Relative to SQ	**1.00**	**1.06**	**1.27**
Cytosine	**SQ**	**MQ1**	**MQ2**
C15	0.62	1.21	1.00
C26	0.71	0.84	1.00
C38	0.77	0.87	1.00
C39	0.58	0.91	1.00
Average	**0.67**	**0.96**	**1.00**
Relative to SQ	**1.00**	**1.46**	**1.50**
Uracil	**SQ**	**MQ1**	**MQ2**
U16	0.95	0.82	1.00
U24	0.81	0.84	1.00
U29	0.88	0.99	1.00
U25	0.89	0.61	1.00
Average	**0.88**	**0.81**	**1.00**
Relative to SQ	**1.00**	**0.93**	**1.14**
Total	**0.70**	**0.89**	**1.00**
Relative to SQ	**1.00**	**1.27**	**1.42**

MQ1: 180(H1′) pulses centered at 5.4 ppm.
MQ2: 180(H1′) pulses centered at 5.7 ppm.

ple quantum coherences $2H1'_xC1'_y$ and $2H6/8_xC6/8_y$ are subject to evolution due to proton chemical shift and spin–spin interactions of H1′ and H6/H8 to nuclei other than C1′ and C6/8. These additional interactions must be refocused to avoid sensitivity loss due to the undesired coherence transfers. In the MQ_ns pulse scheme the refocusing is achieved by inserting two non-selective proton 180° pulses in the middle of the 2Δ evolution period (Marino et al., 1997). Note that a single proton 180° pulse in the middle of the 2Δ period would lead to the evolution being affected also by long-range proton–carbon interactions therefore lowering the conversion to the $4H1'_zC1'_zN1/9_y$, $4H8_zC8_zN1/9_y$ and $4H6_zC6_zN1/9_y$ terms. By using a pair of pulses, all of the heteronuclear couplings are effectively refocused. However, the proton homonuclear interactions H1′–H2′ in sugars and H5–H6 in pyrimidines remain active. Since the coupling constant $J_{H1'H2'} \sim 1$–3 Hz is very small for sugars with

the C3′-*endo* conformation commonly found in A-RNA, the effect of H1′-H2′coupling is not so dramatic. However, a substantial loss in sensitivity is expected for H1′–N1/9 crosspeaks in those residues that are in C2′-*endo* conformation ($J_{H1'H2'} \sim 7$–10 Hz). Such residues are frequently found in non-duplex parts of RNA and predominate in B-DNA structures. A similar loss in sensitivity is anticipated for H6–N1 crosspeaks ($J_{H6H5} \sim 8$ Hz). Examination of Figure 3 confirms that this is exactly the case. Many of the crosspeaks in the pyrimidine region of the MQ_ns spectrum (Figure 3b) are missing and the intensities of the H1′–N9 crosspeaks (Figure 3a) of G_{11}, A_{12} and G_{34} are greatly reduced. G_{11} and A_{12} are located in the internal loop and G_{34} in the bulge of the ATP binding aptamer and their sugar residues adopt C2′-*endo* conformations with $J_{H1'H2'}$ coupling constants of 9.5, 7.8 and 9.0 Hz, respectively (Jiang et al., 1996). The spin-lock experiment efficiently prevents the evolution due to the proton chemical shift and heteronuclear spin–spin interactions. However, concurrent proton–proton Hartman–Hahn (TOCSY) transfer can reduce the attainable sensitivity. As discussed previously (Bax et al., 1985), the amount of transferred magnetization depends strongly on the intensity of the spin-lock field, the transmitter frequency, as well as on the difference in the chemical shifts of the coupled protons. In situations where the coupling constant is large (7–10 Hz) and the difference of chemical shifts small, the interference of Hartman-Hahn transfer cannot be avoided. Portions of the H1′ and H6 signals converted into $2H1'_yH2'_y$ and $2H6_y$ $H5_y$ coherences are inevitably lost during spin manipulations (Sklenář et al., 1998). The sensitivity loss is prevented by using the band-selective pulses to decouple the proton H1′–H2′and H6–H5 interactions (Figure 1). Ideally, the pulses should cover the H1′ and H6/8 regions simultaneously while leaving any coupled protons, especially H2′ and H5, untouched. Unfortunately, the H1′ and H5 regions overlap in nucleic acids (5.3–6.3 ppm). For this reason, the MQ_sel experiment cannot provide optimal performance for both sugar and base protons at the same time and two separate experiments with 180° pulses covering the range of H1′(**Hs**C**Nb**) or H8/H6 (**Hb**C**Nb**) protons are required to achieve the highest sensitivity. As shown in Figure 3 and Table 1, a dramatic gain in sensitivity has been attained.

The **Hs**CNC**Hb** experiment is an *all-the-way-through* experiment as opposed to the *out-and-back* **Hs**/**Hb**C**Nb** experiments. This implies that before the magnetization transfer from C1′ to N1/9 the antiphase $2H1'_zC1'_y$ coherence must be refocused into the C1′ in-phase magnetization. In the original SQ pulse sequence this can be easily done concurrently with the evolution of the $C1'_xN1/9_z$ coherence during the interval 2Δ. The desired magnetization transfer pathway is as follows:

$$\begin{aligned} H1'_z \;&\rightarrow\; H1'_y \rightarrow 2H1'_xC1'_z \rightarrow 2H1'_zC1'_y \\ &\rightarrow\; 2C1'_yN1/9_z \rightarrow 2C1'_zN1/9_y \\ &\rightarrow\; 2C6/8_zN1/9_y \rightarrow 2C6/8_yN1/9_z \\ &\rightarrow\; 2H6/8_zC6/8_y \rightarrow H6/8_y \end{aligned}$$

As discussed above, there is a significant advantage in generating $2H1'_xC1'_y$ coherence during the 2Δ period because of reduced spin–spin relaxation. In the multiple-quantum experiment (Figure 2), the single-quantum antiphase coherence $2H1'_zC1'_x$ is created only briefly at the end of the 2Δ period to allow refocusing of the $4H1'_zC1'_yN9/1_z$ into $2C1'_xN9/1_z$ magnetization. Similar to the **Hs**/**Hb**C**Nb** experiment, all of the possible homonuclear and heteronuclear interactions of H1′ must be refocused during the interval 2Δ. This has been achieved by inserting two H1′ band-selective proton 180° pulses in the middle of the Δ periods. The selective 180° C1′ carbon pulse is shifted by δ to the center of the $2\Delta + 2\delta$ interval to provide concurrent refocusing of the $2H1'_zC1'_x$ antiphase coherence. The other half of the pulse sequence is a mirror image of the first one with the evolution intervals now set to correspond to the coupling constants in purine and pyrimidine bases. The band-selective proton 180° pulses effectively decouple proton–proton and proton–nitrogen interactions. Since the multiple-quantum $2H1'_zC1'_x$ coherence does not evolve due to $J_{H1'C1'}$ coupling, the shifting of the C1′ carbon refocusing pulse by a time interval δ has no detrimental effect on this coherence as long as the chemical shifts of both proton and carbon are refocused. However, this arrangement makes the evolution intervals longer by 2δ and does not completely remove the effect of long-range carbon–proton interactions on the C1′ magnetization. This contributes to the fact that the sensitivity increase in this experiment is not as dramatic as with the **Hs**/**Hb**C**Nb** experiment. Furthermore, extending the refocusing in H1′ region upfield to 4.4 ppm also affects many H2′ protons, thus compromising the performance of the experiment (MQ1 in Table 2). We observed a drop in overall sensitivity by about 10% as a result of this. In addition, relaxation behavior is also not uniform, and different correla-

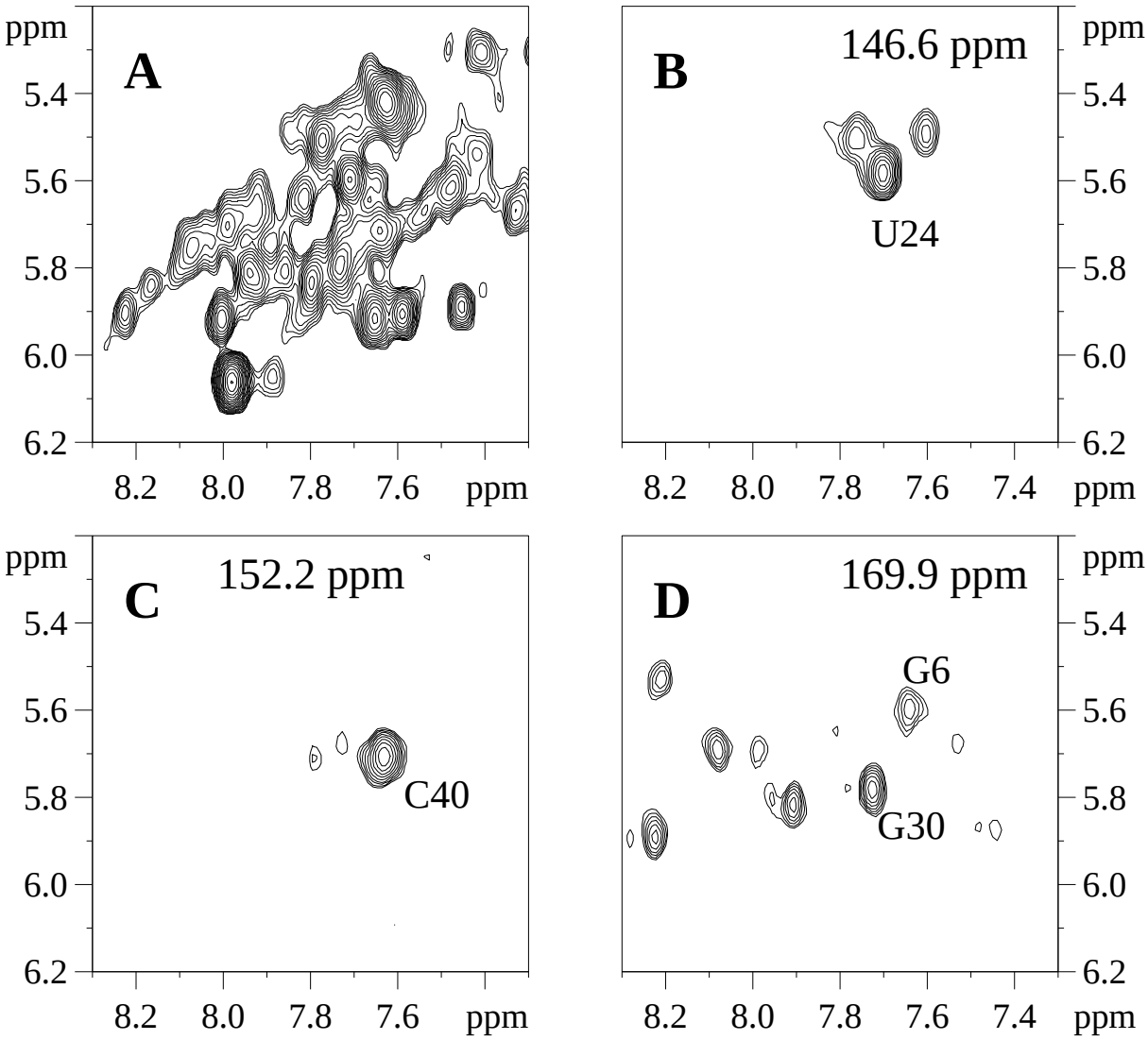

Figure 5. Severely overlapped peaks in a crowded region of the 2D **Hs**CNC**Hb** spectra (A) are easily resolved in a 3D **Hs**C**Nb**C**Hb** version of the experiment with chemical shift correlation of glycosidic nitrogens N1/9 in the third dimension (B)–(D). The number in the upper right hand corner shows ^{15}N chemical shift of the plane. Spectra were collected using 40 × 24 × 256 complex points for the spectral widths of 3.05 ppm, 30.1 ppm, and 5.0 ppm in F1, F2, and F3 dimensions, respectively, with 16 scans per t_1 and t_2 increment. Total acquisition time was 24 h.

tion times are expected for the double helical section, the bulge and loop of the ATP binding aptamer complex. Nevertheless, several peaks that were missing in the single quantum experiment showed up clearly in the multiple-quantum version. An average increase in the sensitivity of the optimally adjusted multiple-quantum **Hs**CNC**Hb** experiment was 78% for adenine, 27% for guanine, 50% for cytosine and 14% for uracil nucleotides (Table 2). We have found that in addition to sensitivity, peak overlap becomes a problem in resolving the **Hs**CNC**Hb** spectra of the RNA aptamer complex with 40 nucleotides. The cause is the relatively narrow distribution of the proton chemical shifts. Converting the experiment into a 3D one, with the ^{15}N chemical shift labeling in the third dimension, proved very helpful in resolving the overlapped peaks (Figure 5). Unlike the sugar H1′ protons and base H6/H8 protons and C6/8 carbons, glycosidic nitrogens N1 of cytosine (150–154 ppm) and uracil (143–148 ppm) and N9 of purines (160–175 ppm) are found in very distinct spectral regions.

Conclusions

We have shown that the use of multiple-quantum coherence for reducing spin–spin relaxation in combination with careful control of coherence transfer processes greatly improves the efficiency of the experiments for sugar-to-base correlation in labeled oligonucleotides. The optimized multiple-quantum **Hs**/**Hb**C**Nb** experiments achieve a substantial gain in sensitivity over a non-selective one both in the sugar (50%) and base (200–400%) region. In addition, these experiments will be applicable to fully labeled DNA oligonucleotides with a predominantly C2′-*endo* conformation. The multiple-quantum **Hs**C**Nb**C**Hb** experiment with an average gain in sensitivity of 42% over the single-quantum experiment enabled us to obtain a high quality 3D spectrum of a 40mer RNA complex within 24 h. Thus, the experiments described present an improved tool for NMR studies of larger $^{13}C/^{15}N$ labeled RNA and DNA oligonucleotides.

Acknowledgements

The research has been supported partially by the Grant Agency of the Czech Republic, Grant No. 203/96/1513 and by the Ministry of Education of the Czech Republic, Grant No. VS 96095. We thank Dr. Dinshaw Patel of Memorial Sloan-Kettering Cancer Center for the sample of ATP-binding RNA aptamer used in this study.

References

Batey, R.T., Inada, M., Kujawinski, E., Puglisi, J.D. and Williamson, J.R. (1992) *Nucleic Acids Res.*, **20**, 4515–4523.

Bax, A. and Davis, D.G. (1985) *J. Magn. Reson.*, **65**, 355–360.

Farmer, B.T., Müller, L., Nikonowicz, E.P. and Pardi, A. (1993) *J. Am. Chem. Soc.*, **115**, 11040–11041.

Farmer, B.T., Müller, L., Nikonowicz, E.P. and Pardi, A. (1994) *J. Biomol. NMR*, **4**, 129–133.

Fiala, R., Jiang, F. and Patel, D.J. (1996) *J. Am. Chem. Soc.*, **118**, 689–690.

Geen, H. and Freeman, R. (1991) *J. Magn. Reson.*, **93**, 93.

Griffey, R.H. and Redfield, A.G. (1987) *Q. Rev. Biophys.*, **19**, 51–82.

Grzesiek, S. and Bax, A. (1995) *J. Biomol. NMR*, **6**, 335–339.

Heus, H.A., Wijmenga, S.S., van de Ven, F.G.M and Hilbers, C.W. (1994) *J. Am. Chem. Soc.*, **116**, 4983–4984.

Ippel, J.H., Wijmenga, S.S., de Jong, R., Heus, H. A., Hilbers, C.W., de Vroom, E., van der Marel, G.A. and van Boom, J.H. (1996) *Magn. Reson. Chem.*, **34**, 156–176.

Jiang, F., Fiala, R., Live, D., Kumar, R.A. and Patel, D.J. (1996) *Biochemistry*, **35**, 13250–13266.

Marino, J.P., Schwalbe, H., Anklin, C., Bermel, W., Crothers, D.M. and Griesinger, C. (1994) *J. Am. Chem. Soc.*, **116**, 6472–6473.

Marino, J.P., Schwalbe, H., Anklin, C., Bermel, W., Crothers, D.M. and Griesinger, C. (1995) *J. Biomol. NMR*, **5**, 87–92.

Marino, J.P., Diener, J.L., Moore, P.B. and Griesinger, C. (1997) *J. Am. Chem. Soc.*, **119**, 7361–7366.

Michnicka, M.J., Harper, J.W. and King, G.C. (1993) *Biochemistry*, **32**, 395–400.

Nikonowicz, E.P., Sirr, A., Legault, P., Jucker, F.M., Baer, L.M. and Pardi, A. (1992) *Nucleic Acids Res.*, **20**, 4507–4513.

Ramachandran, R., Sich, C., Grüne, M., Soskic, V. and Brown, L.R., (1996) *J. Biomol. NMR*, **7**, 251–255.

Sassanfar, M. and Shostak, J.W. (1993) *Nature*, **364**, 550–553.

Shaka, A.J., Barker, P. and Freeman, R. (1985) *J. Magn. Reson.*, **64**, 547.

Simorre, J.-P., Zimmermann, G.R., Pardi, A., Farmer II, B.T. and Mueller, L. (1995) *J. Biomol. NMR*, **6**, 427–432.

Simorre, J.-P., Zimmermann, G.R., Mueller, L. and Pardi, A. (1996) *J. Biomol. NMR*, **7**, 153–156.

Simorre, J.-P., Zimmermann, G.R., Mueller, L. and Pardi, A. (1996a) *J. Am. Chem. Soc.*, **118**, 5316–5317.

Sklenář, V., Peterson, R.D., Rejante, M.R., Wang, E. and Feigon, J. (1993) *J. Am. Chem. Soc.*, **115**, 12181–12182.

Sklenář, V., Peterson, R.D., Rejante, M.R. and Feigon, J. (1993a) *J. Biomol. NMR*, **3**, 721–727.

Sklenář, V., Dieckmann, T., Butcher, S.E. and Feigon, J. (1996) *J. Biomol. NMR*, **7**, 83–87.

Sklenář, V., Dieckmann, T., Butcher, S.E. and Feigon, J. (1998) *J. Magn. Reson.*, **130**, 119–124.

Sörensen, O.W., Eich, G.W., Levitt, M.H., Bodenhausen, G. and Ernst, R.R. (1983) *Prog. NMR Spectrosc.*, **16**, 163–192.

Tate, S., Ono, A. and Kainosho, M. (1994) *J. Am. Chem. Soc.*, **116**, 5977–5978.

Tate, S., Ono, A. and Kainosho, M. (1995) *J. Magn. Reson.*, **B106**, 89–91.

Varani, G., Aboul-ela, F., Alain, F. and Gubster, C.C. (1995) *J. Biomolecular NMR*, **5**, 315–320.

Wijmenga, S.S., Heus, H.A., Leeuw, H.A.E., Hope, H., van der Graaf, M. and Hilbers, C.W. (1995) *J. Biomol. NMR*, **5**, 82–86.

Wüthrich, K. (1986) *NMR of Proteins and Nucleic Acids*, Wiley, New York, NY.